Flux Variations in GeV and TeV Blazar Light Curves

Sarah M. Wagner,[a,b] P. R. Burd,[a] S. Buson,[a] D. Dorner,[a] A. Gokus,[a,c] G. Madejski,[b] K. Mannheim,[a] and J. D. Scargle[d]
on behalf of the *Fermi*-LAT and FACT Collaborations ([a] University of Würzburg; [b] KIPAC and SLAC, [c] Remeis-Observatory/ECAP; [d] NASA Ames)

Motivation and Data

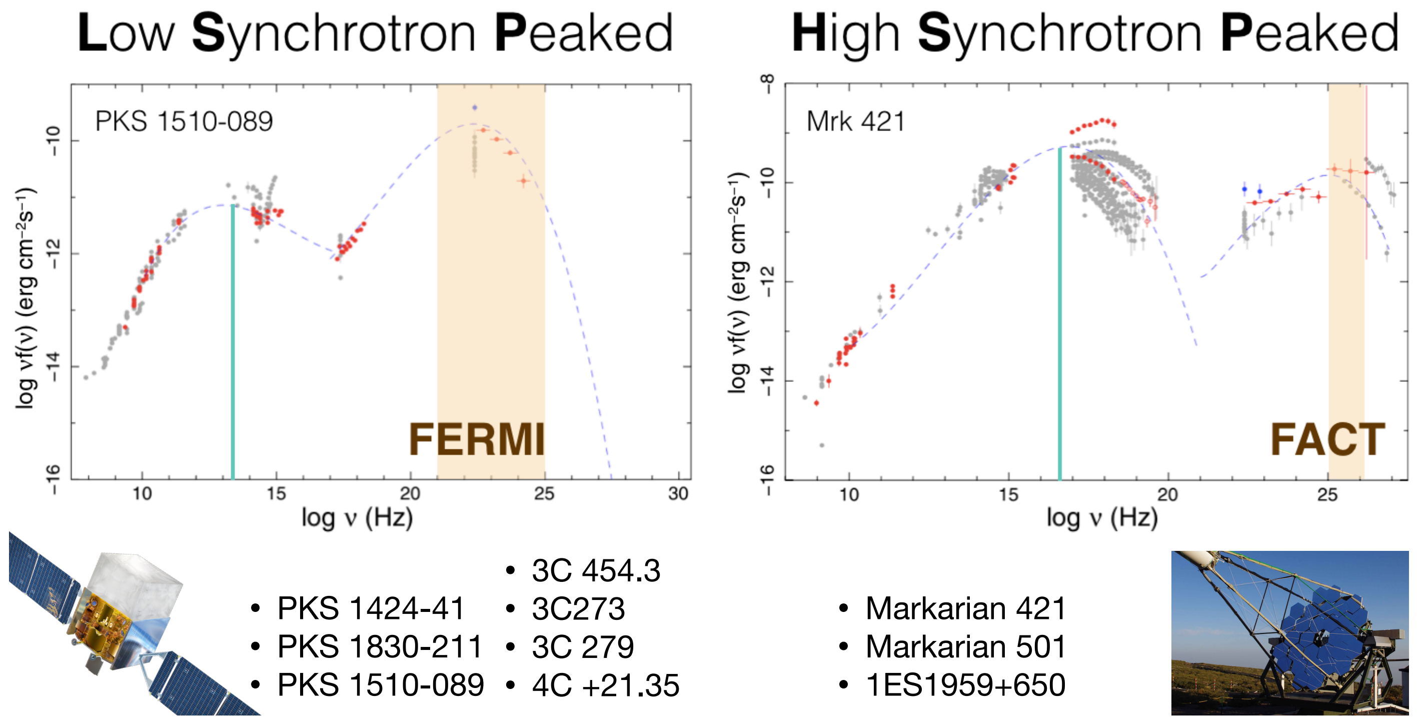

Figure 1: Based on the peak position of the low energy hump (cyan line) in the spectral energy distribution, blazars can be classified as low- and high-synchrotron peaked objects (LSP and HSP), as shown for PKS 1510-089 and Mrk 421, respectively. The intrinsic difference between these classes as well as the processes responsible for the high-energy hump remain uncertain. Thus, we analyze the high-energy variability with *Fermi*-LAT and FACT (bottom left and right) which cover the respective high-energy hump for the brightest LSP and HSP sources as listed below the SEDs.

Data analysis *Fermi*-LAT:

- time: 2008-08-05 to 2020-12-31
- energy: 100 MeV to 300 GeV
- only flux bins with TS>4 and flux error < flux
- standard analysis (see proceedings article)

Data analysis FACT:

- time: 2011-11-15 to 2020-01-23
- energy: above 300 GeV
- light curve divided into chunks (seasonal gaps)
- standard analysis (see proceedings article)

Conclusions

- Daily binned GeV (*Fermi*-LAT) as well as TeV (FACT) flares determined with HOP algorithm result in:
  - Large fraction of single block flares → suggests flux variations take place on intra-day timescales
  - No preferred asymmetry for flares with more than one block
- High-energy flux fluctuations could, for instance, be produced by one or several plasmoids moving along the jet [3]
- Ornstein-Uhlenbeck parameter extraction indicates that amplitude of random fluctuations differs for the samples considered

Keywords

(very) high-energy γ-ray, blazars, variability, flare asymmetry, time series analysis, stochastic (Ornstein-Uhlenbeck) process

Variability Analysis

- Characterize flares with the HOP algorithm as shown in Fig. 2, following [1]
  1. Apply the Bayesian block algorithm
  2. Peak time = center of local maximum
  3. Subsequently lower blocks belong to peak (watershed method)
  4. Define start and end time of a flare; similar results (Fig. 3 and Fig. 4) for either method
     (a) *baseline*: Determined by flux exceeding/dropping under certain flux level (e.g. quiescent background)
     (b) *half*: Divide valley blocks in half
     (c) *sharp*: Neglect valley blocks
     (d) *flip*: Extrapolate slope of flare by flipping length of adjacent block onto valley block → this work

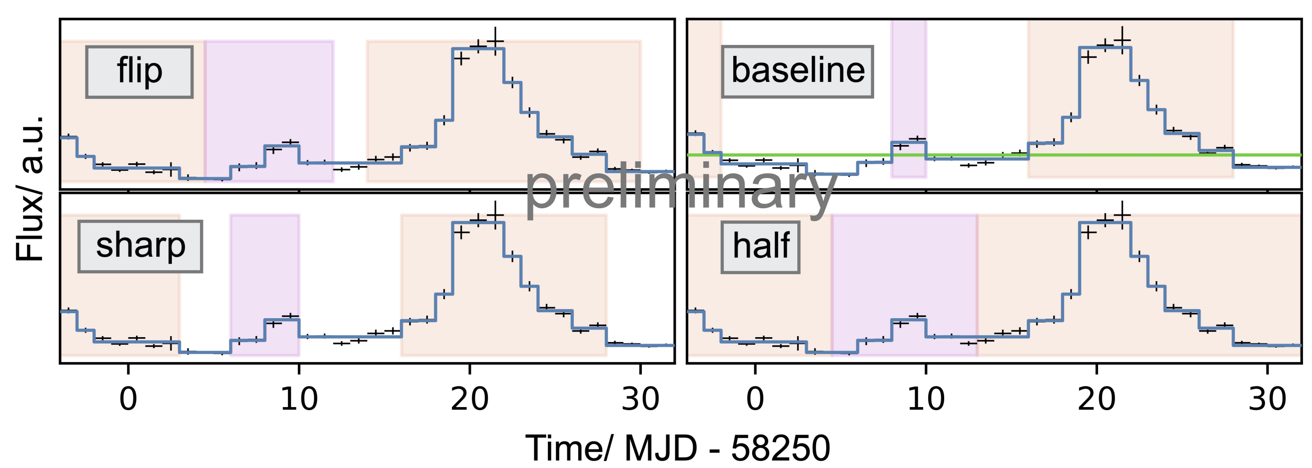

Figure 2: Based on Bayesian blocks (blue) and corresponding method, we define flares (orange and purple) in the daily binned light curves (here: *Fermi*-LAT, 3C 279).

- Extract OU parameters of each light curve [2] Assume flux variations are correlated noise parametrized by a first order auto-regressive process; the discrete OU process (see Eq. 5e in [2])

$$u_{T+1} = u_T + \theta \Delta t(\mu - u_T) + \sigma \sqrt{\Delta t} \mathcal{N}_T \quad (1)$$

→ μ = mean revision level, θ = mean revision rate
→ White noise implemented with independent draws from normal distribution $\mathcal{N}(m = 0, \sigma^2)$
→ Value of the time series u_T is logarithm of flux

Results

47% (*Fermi*-LAT) and 48% (FACT) of all flares consist of a single block indicating shorter variability that is not resolved in daily binning. We exclude these flares and compute for all remaining flares the asymmetry measure

$$A = \frac{t_{\mathrm{rise}} - t_{\mathrm{decay}}}{t_{\mathrm{rise}} + t_{\mathrm{decay}}} \quad (2)$$

with t_{rise} and t_{decay} determined by the start, peak, and end time. The probability density for A is shown in Fig. 3.

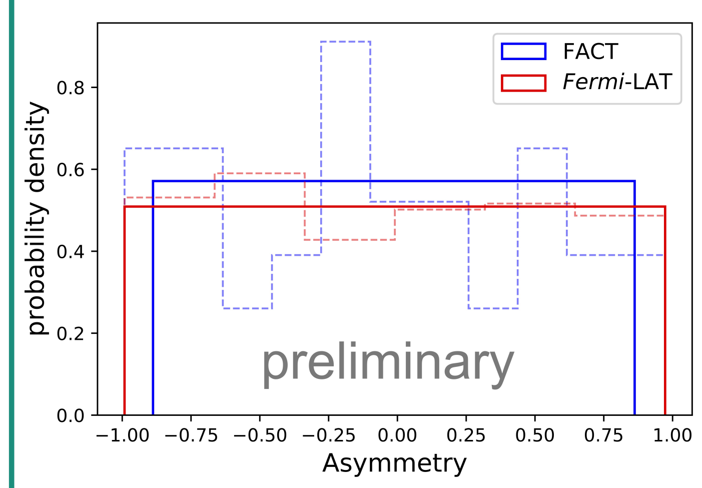

Figure 3: Probability density for asymmetry measures of *Fermi*-LAT and FACT flares in constant (dashed line) and Bayesian binning (solid line).

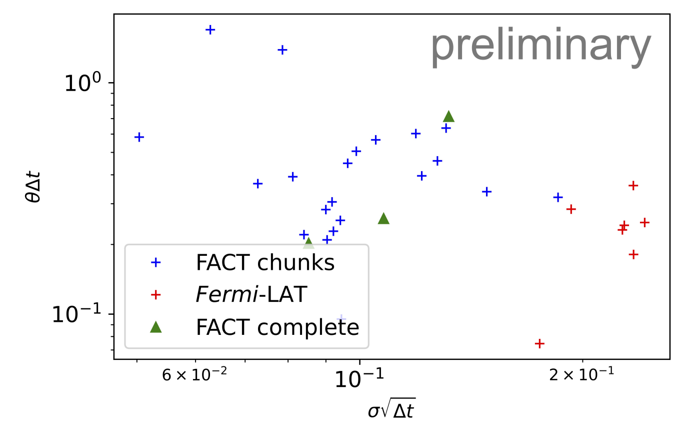

Figure 4: Scatter plot of the extracted OU parameters σ and θ for the *Fermi*-LAT light curves and FACT chunks (as analyzed before) as well as the complete FACT light curves.

We obtain two statistically equivalent, flat distributions, ranging from -1 to $+1$, meaning that each kind of asymmetry occurs to a comparable degree and we do not find differences between the two samples.

The extracted OU parameters σ and θ are shown in Fig. 4. The former clearly differs for the LSP and HSP sources (*Fermi*-LAT and the FACT chunks/light curves, respectively).

References

[1] M. Meyer, J. D. Scargle and R. D. Blandford, *Characterizing the Gamma-Ray Variability of the Brightest Flat Spectrum Radio Quasars Observed with the Fermi LAT*, ApJ **877** (2019) 39 [1902.02291].

[2] P. R. Burd, L. Kohlhepp, S. M. Wagner, K. Mannheim, S. Buson and J. D. Scargle, *Ornstein-Uhlenbeck parameter extraction from light curves of Fermi-LAT observed blazars*, **645** (2021) A62 [2010.12318].

[3] M. Meyer, M. Petropoulou and I. M. Christie, *The Observability of Plasmoid-powered γ-Ray Flares with the Fermi Large Area Telescope*, **912** (2021) 40 [2012.09944].

Contact Information

GitHub github.com/swagner-astro

Email sarah.wagner@physik.uni-wuerzburg.de